

# EXPERIMENTAL STUDY OF THE INTERNAL EROSION BEHAVIORS OF GRANULAR SOILS IN HORIZONTAL SEEPAGE

## EKSPERIMENTALNA ŠTUDIJA NOTRANJE EROZIJE GRANULIRANE ZEMLJINE MED HORIZONTALNIM PRONICANJEM VODE

Yue Liang<sup>1,2</sup>, Zhiwei Sun<sup>1,2\*</sup>, Qiang Zhang<sup>3</sup>

<sup>1</sup>National Engineering Research Center for Inland Waterway Regulation, Chongqing Jiaotong University, Chongqing, China

<sup>2</sup>School of River and Ocean Engineering, Chongqing Jiaotong University, Chongqing, China

<sup>3</sup>Dongxing District Water Resources Bureau, Neijiang, China

*Prejem rokopisa – received: 2021-09-25; sprejem za objavo – accepted for publication: 2021-12-29*

doi:10.17222/mit.2021.274

Internal erosion is one of the most common failure mechanisms in hydraulic structures. The internal erosion is generally initiated by horizontal seepage in earth-filled embankments such as levees. With a newly developed apparatus we carried out a set of internal erosion experiments in horizontal seepage. The experiments used gap-graded granular soil to prepare the specimens. The experimental results revealed that, in a horizontal column, the upper part of the specimen is preferentially eroded, sequentially forming a dominant seepage area. When the erosion progresses, the dominant seepage area gradually expands from the upper part to the lower part of the column. At the particle scale, the localized fine-particle movement can be observed in the erosion process when the hydraulic gradient is relatively small, e.g., less than 0.62. During the early stage of erosion, the particles are rapidly eroded. With the erosion time increasing, the particle loss slows down and even ceases if there is sufficient time.

Keywords: internal erosion, horizontal seepage, dominant seepage area, hydraulic gradient.

Interna erozija je eden najbolj pogostih mehanizmov poškodb ali porušitve hidravličnih struktur. V glavnem se notranja erozija (odplavljanje delcev) začne s horizontalnim pronicanjem kapljevine v zemljinah, kot so naprimer rečni nasipi. Avtorji v članku opisujejo novo razvit aparat s katerim so lahko izvedli vrsto preizkusov horizontalnega pronicanja. Za preizkuse so pripravili preizkušance iz zemljine s kontrolirano granulacijo. Izvedeni preizkusi so pokazali, da v horizontalnem stebričku erodira predvsem zgornji del preizkušanca, kar vodi v nastanek prednostnega področja pronicanja. Ko erozija napreduje se prevladujoče področje erozije postopno razširja iz zgornjega dela stebrička tudi na njegov spodnji del. Na velikostni skali delcev zemljine so opazili lokalno gibanje finih delcev med procesom erozije že pri relativno majhnem hidravličnem gradientu; to je, ko je bil le ta manjši od 0,62. Že v zgodnjem stadiju erozije delci hitro erodirajo oziroma jih hitro odplavlja (odnaša). Z nadaljevanjem erozije se izguba delcev zmanjšuje in celo preneha, če je za to dovolj časa.

Ključne besede: notranja erozija, horizontalno pronicanje, prevladujoče področje pronicanja, hidravlični gradient

## 1 INTRODUCTION

Internal erosion is one of the leading causes of failure in hydraulic engineering structures. Statistically, 46.1 % of dam failures worldwide are caused by internal erosion.<sup>1-3</sup> The two-stratum dyke structure, commonly found in the Yangtze River dyke system, is generally composed of a weakly permeable overburden and an underlayer with high permeability. This special strata is prone to causing internal erosion.<sup>4</sup>

Many scholars have carried out studies on internal erosion. For example, Liang<sup>7</sup> and Chen<sup>8</sup> found that the direction of internal erosion changes from vertical to horizontal, which accelerates the failure of the upper soil layer. Vandenboer<sup>9</sup> and Ni<sup>10</sup> explored the characteristics and structure of sand layer materials via particle size analysis. They found that erosion failure begins with the loss of fine particles around the erosion outlet. Cao<sup>11</sup> and Xiao<sup>12</sup> analyzed the migration of particles at the tip of

the channel through the erosion failure test of one-dimensional vertical upward seepage. The present research enhances our understanding of internal erosion. However, these researches mainly focus on the internal erosion, vertical seepage. The erosion in the horizontal seepage flow is insufficiently concerned.<sup>13,14</sup> The internal erosion is easier to initiate since the direction of gravity is no relevant. Research on the seepage of soil show that the dominant direction of the seepage is usually horizontal. The capability to resist the horizontal internal erosion is lower than the vertical.<sup>15-17</sup> Therefore, it is crucial to research particle movement under horizontal seepage conditions to prevent the dyke.

In this research we design a new apparatus to investigate the migration of particles under internal horizontal erosion. The gap-graded granular soil is used to prepare the specimens. The particles are dyed to trace the eroding process. The order and direction of the migration of the filled fine particles in the specimens are realized. The sand gushing at the erosion outlet and the loss of particles in the specimen are recorded by a camera to study

\*Corresponding author's e-mail:  
sunzhiwei\_0915@163.com (Zhiwei Sun)

the erosion behavior of fine particles in horizontal seepage.

## 2 EXPERIMENTAL PART

### 2.1 Materials

The materials used in this study were collected from the Yangtze River beach in Chongqing, China. The materials were washed with distilled water to eliminate the clay particles and impurities. Then, following the process outlined by the ASTM<sup>18</sup>, particles with diameters ranging from 0.075 mm to 10.0 mm were isolated using the sieving method. Finally, these selected particles were classified into different groups according to the diameter, i.e., (10–8; 8–5; 5–3; 3–2; 2–1; 0.25–0.075) mm.

The specimen preparation followed a given particle size distribution (PSD) shown in **Figure 1**. The PSD indicates the materials are gap-graded with the particles of 0.25–1.0 mm excluded. The geometric and mechanic properties of the particles used in this study are listed in **Table 1**.

**Table 1:** Geometric and mechanic properties of soils used for specimen preparation

$D_{15}/\text{mm}$	$d_{85}/\text{mm}$	$P/\%$	$C_u/\text{mm}$	$G_s$	$\rho/(\text{g}/\text{cm}^3)$
3.4	0.224	20	40.9	2.67	1.92

Abbreviations:  $D_{15}$  – diameter of the 15 % mass passing in the coarse component;  $d_{85}$  – diameter of the 85 % mass passing in the fine component;  $P$  – fine particle content;  $C_u$  – coefficient of uniformity;  $\rho$  – dry density;  $G_s$  – specific gravity

The cumulative mass of fine particles (0.25–0.075 mm particle size group) accounts for 20 % of the total sample mass. The content of the fine particles is below the critical content for filling the voids between coarse particles in a gap-graded soil.<sup>19</sup> This implies that the soil is internally unstable following the criteria proposed by Liang et al.<sup>20</sup> Fine particles in the specimen can migrate into pores composed of coarse particles under the seepage ac-

tion. The fine particles are dyed to trace their movement with diameters from 0.25 mm to 0.075 mm. The dye colors used in this study are green, blue, and red, as shown in **Figure 2**. Additionally, a group of fine particles remains in the original color, i.e., grey.

### 2.2 Apparatus

We designed a new apparatus to investigate the migration of particles under internal horizontal erosion.<sup>21</sup> As shown in **Figure 3**, this apparatus consists of a soil-water separating system, a specimen container, a water-supply system, a data-acquisition system, and some piezometers. The specimen container is made of a polymethyl methacrylate (PMMA) tube. The inner diameter and the thickness of the tube are 100 mm and 10 mm, respectively, and its length is 500 mm. The specimen is directly prepared in the PMMA tube, and the intact specimen is 320 mm long before being eroded during the experiment. The specimen is supported by a bottom steel plate in the container. This plate, with a thickness equal to 5 mm, is perforated with holes of 5.0 mm in diameter. The interval between holes is equal to 6.0 mm. On the plate, a steel wire sieve with 75.0- $\mu\text{m}$  holes is installed to prevent falling out of the fine particles of the specimen. These holes provide uniform water flow to the bottom of the specimen in the experiment. An air cylinder is located at the bottom of the specimen container and exerts stable axial pressure on the specimen to simulate the static earth pressure state. The front and rear brackets are used to fix the specimen container and the cylinder. Six piezometers are arranged with the same interval on the sidewall of the container to monitor the water head along the specimen. The water-supply system consists of an elevation-adjustable water tank. The tank provides the required hydraulic gradient by lifting the height of the water tank. The soil-water separating system collects and separates the water and the eroded particles flowing out of the specimen from the top of the column. The sand-carrying water flows through the conduit

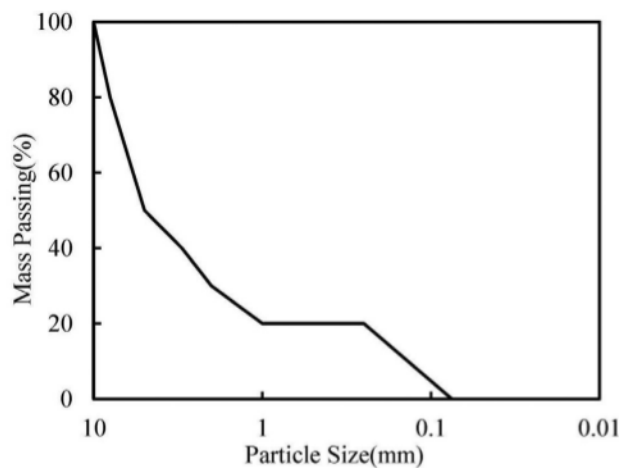


**Figure 1:** Particle size distribution

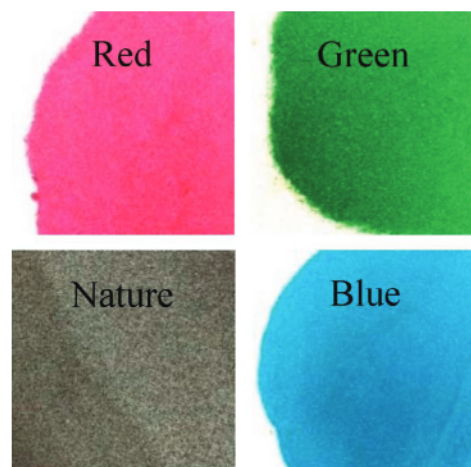


**Figure 2:** Four color particles



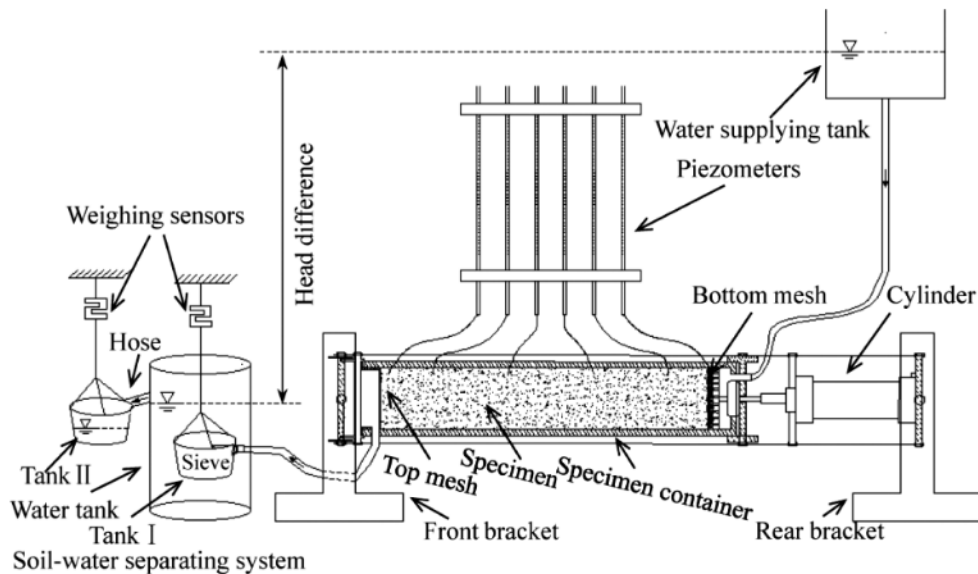


Figure 3: Sketch of the apparatus used in this study

into Tank I, which can separate the particles from the water. The fine particles sink into the bottom due to gravity. The sieve is placed at the bottom of Tank I, and fine particles accumulate at the bottom. The weighing sensors record the amount of particle loss in the experiment. The water level in Tank I is the same height as the hose, letting the excess water spill into the Tank II freely. A weighing sensor monitors the weight of Tank II. From the change of weight, the flux through the specimen can be calculated.

### 2.3 Experiment procedure

The testing scheme includes the following procedures. The first step of the experiment is the preparation of the specimen. The particles with different sizes are chosen proportionally, following the given PSD. Before loading the particles into the specimen container, the specimen container is set to a vertical position. The length of the specimen is 320 mm, and the filling height of each colored specimen section is 80 mm. To prevent the segregation of different sized particles, the wet ramming method is used to fill the specimen layer by layer.<sup>22</sup> The height of each layer is 20 mm. The specimen is filled 16 times. The dry density is controlled to 1.92 g/cm<sup>3</sup>. The total mass of the specimen is 4900 g, and the mass of colored fine particles is 980 g. The second step is to adjust the angle of the specimen container. When the specimen preparation is completed, we adjust the front and rear brackets to ensure the specimen container is horizontal. The third step is to apply the desired stress. The horizontal axial stress, equal to 120 kPa, is applied to the specimen to simulate a static earth-pressure state. The stress is from the cylinder connecting to a constant-pressure air source. The axial deformation is recorded to determine the volumetric strain of the specimen after the pressure is applied. The fourth step is to

saturate the specimen for at least 4 h to ensure the full saturation of the specimen. The fifth step is capturing the critical hydraulic gradient of the internal erosion. By lifting the water-supplying tank height to increase the hydraulic gradient. We control the increment rate of the hydraulic gradient at about 0.005 per minute. After the sustained erosion is initiated, the increase of the hydraulic gradient is terminated. The final step is to investigate the erosion process in the specimen. In this step we use a different constant hydraulic gradient to investigate the effects of the hydraulic gradient on the erosion behaviors. During the test, the weighing sensor and the digital camera monitor the loss of fine particles and the change of the specimen coloring area in real-time.

## 3 RESULTS

### 3.1 Progression of the erosion

Figure 4 shows the appearances of the specimen at different stages during the erosion. Figure 4a is the specimen before the erosion. Particles with four different colors fill the specimen. The specimen with the original color, green, red, and blue, are labeled as Sections I, II, III, and IV, respectively. The axial deformation is 0.03 mm in the specimen after applying a 120-kPa horizontal axial stress. Figure 4b to 4d are photographs of specimens when the erosion time reaches (161; 201; 512) min, respectively. The color change of the specimen surface indicates that the colored fine particles migrated during the horizontal seepage process. The loss of the fine particles follows the preferential flow paths. The area with more loss of fine particles belongs to the dominant seepage area. The area above the yellow lines in Figure 4b, and 4d experiences the most severe loss of the colored fine particles. In contrast, the area below the yellow line is less affected by the seepage erosion. As

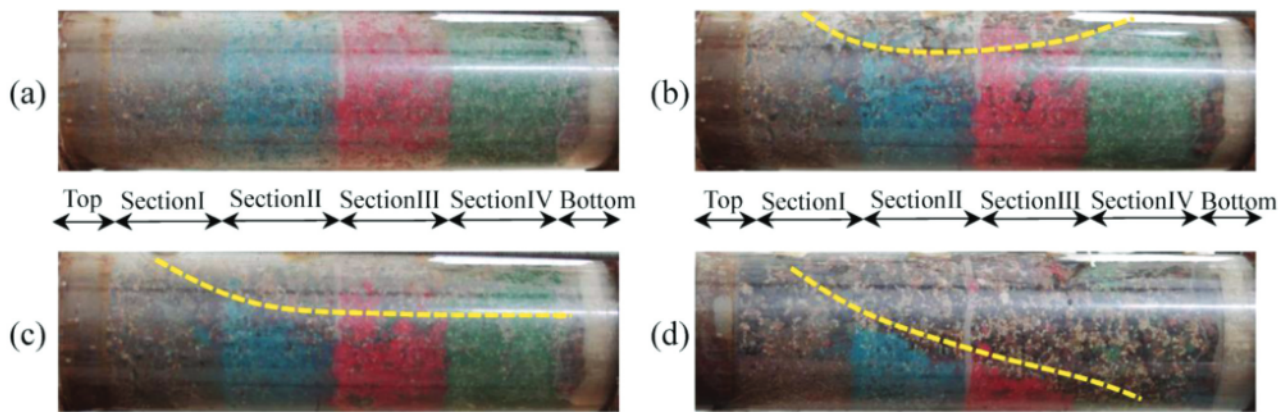


Figure 4: The photographs of different erosion stages

the experiment continues, the fine particles are continuously removed. The prevailing seepage paths merge and form a larger path. The yellow line gradually moves to the lower part of the specimen.

Figure 5a and 5b show the four cross-sections of the specimen at the beginning and end of the test, respectively. Before the test, the colored fine particles of the four cross-sections are evenly distributed, as shown in Figure 5a. After the test, the colors of the four cross-sections change significantly, as shown in Figure 5b. The changes in the cross-section color reflect the degree of

particle loss. The fine particle loss above the red line is the most serious. The colored fine particles almost totally disappeared, indicating complete erosion in this area. Due to the complexity of pore properties and sizes, the fluid motion characteristics within the pores also show a significant divergence. The formation process of the seepage channel is also the process of water finding the weakest link in the soil. Water flow preferentially flows along some paths to form the "dominant flow", which makes the velocity distribution of the seepage field uneven, resulting in an uneven particle loss.

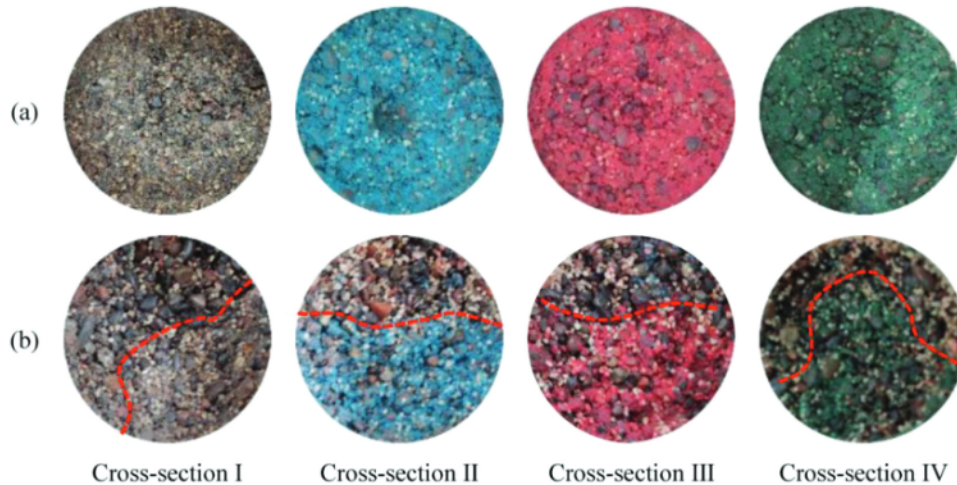


Figure 5: Sections of different erosion stages

Table 2: The accumulation statistics of colored particles in Tank I at different stages of erosion

No.	erosion time (min)	accumulated loss (g)	accumulated loss rate (%)	hydraulic gradient	statistics of accumulation of colored particles in tank I
1	38	0	0	0.4	No particle loss.
2	66.1	0	0	0.62	The upper part of the grey sample section has been moved violently without loss of fine particles.
3	164.7	74.42	7.59	0.92	Mainly blue fine particles, with a small amount of red.
4	207.8	223.26	22.78	1.47	Mainly red fine particles, with a small amount of green.
5	244.3	327.21	33.39	1.78	Mainly green fine particles.
6	349.4	404.0	41.22	1.78	Mainly green fine particles, the particle loss rate decreases.
7	512.7	446.52	45.56	1.78	At the end of the test, there are 45.56 % colored fine particles in the specimen.



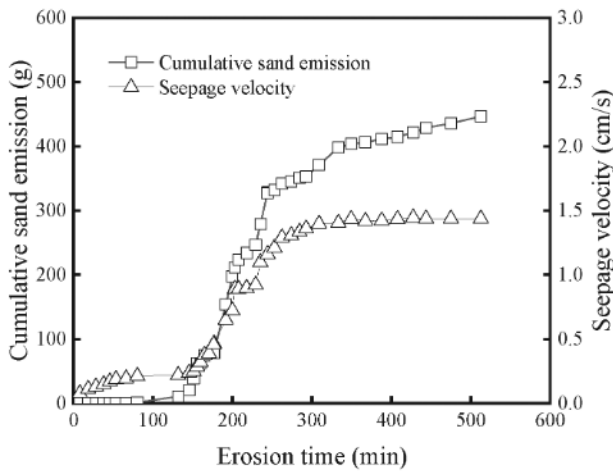


Figure 6: Curve of cumulative particle loss and seepage velocity with erosion time

### 3.2 Fine particle erosion analysis

Table 2 shows the fine particles in Tank I at different erosion stages. Before the hydraulic gradient reaches to 0.4, particles are not eroded from the specimen. When the erosion process lasts about 66.1 min, some fine particles move around their original location, especially in the upper part of the specimen. At this time, the hydraulic gradient is 0.62. The local movement occurs when the particles roll or move up and down in the soil pore, but a few particles are lost. If the hydraulic gradient continues to increase, the global movement and the continuous erosion of the fine particles will be triggered. When the test time reaches 164.7 min, 207.8 min, and 244.3 min, the dominant colors of the eroded particles accumulated in Tank I are blue, red, and green, and the corresponding hydraulic gradients are 0.92, 1.47, and 1.78, respectively. The cumulative loss of fine particles is 446 g, accounting for about 45.5 % of the fine particles.

Figure 6 shows the variations of the cumulative particle loss and the seepage velocity with the increase of the erosion time. In the initial stage of the experiment, from the beginning to an experimental time equal to 66 min, for example, a few eroded fine particles can be observed. Moreover, the seepage velocity changes linearly with the erosion time and the hydraulic gradient, since the water head increases linearly. When experimental time exceeds 66.0 min, particles begin to migrate out of the specimen. And the loss of fine particles represents the start of the internal erosion. During the experimental time from 131.0 min to 349.0 min, the fine particles experience a rapid loss. When the erosion time exceeds 349 min, the loss of the fine particles increases slowly. The value of the permeation flow rate changes imperceptibly. The water flow becomes transparent again if the time is long enough. The particle loss tends to cease.

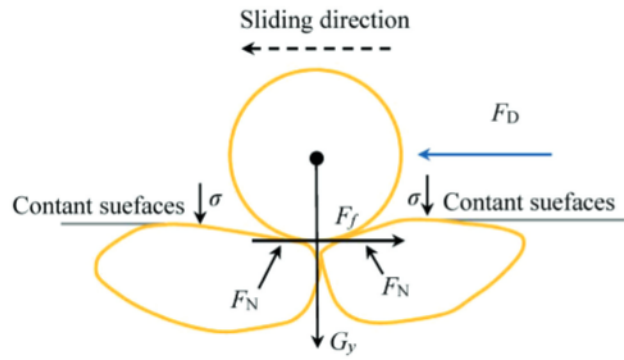


Figure 7: Movable particle force analysis

## 4 DISCUSSION

The essence of internal erosion is the process that the force balance of the particles is destroyed. The PSD of the soil is gap-graded granular soil, since particles with sizes of 0.25–1.0 mm are excluded. Therefore, fine particles are easier to pass through the pores between the coarse particles. According to the theory of sediment incipient motion in horizontal erosion sediment,<sup>23,24</sup> assuming that fine particles are spheres, the forces on the movable particles generally are the drag force  $F_D$ , the uplift force  $F_y$ , the subaqueous particle gravity  $G_y$  and the interparticle friction  $F_f$ . Under horizontal seepage conditions, the role of the uplift force is small and ignorable.<sup>25</sup> The particle force analysis is shown in Figure 7.<sup>16</sup> The expressions of the force are as follows:

$$\begin{cases} G_y = \frac{\pi}{6}(\gamma_s - \gamma_w)D^3 \\ F_f = fF_N \\ F_D = \rho_w \frac{C_x v^2}{2} \frac{\pi}{4} D^2 \end{cases} \quad (1)$$

where  $\rho_w$  is the density of fluid,  $C_x$  is the drag force coefficient,  $D$  is particle diameter,  $v$  is the velocity,  $\gamma_s$  is the volume weight of particles,  $\gamma_w$  is the volume weight of the fluid,  $F_N$  is the particle lateral pressure,  $f$  is the friction coefficient, and  $\sigma$  is the vertical effective stress on contact surface of movable fine grained soil.

When  $F_D > F_f$ , static fine particles transform into particles in motion. The resultant force of the moving particles is inclined downward. That is, the particles move forward and also move downward. The fine particles in the upper part of the specimen are eroded from the pores. And the pores are not supplemented. So, a dominant seepage zone is formed in the upper part of the specimen. The seepage velocity and the particle diameter of the fine particles affect the value of the positive thrust. The smaller the particle diameter is, the easier the particles will be lost. In the early stage of the internal erosion, the number of movable particles is the greatest, so the loss of the particles is severe. As the erosion continues, the particle loss slows down or even stops when the drag

force generated under the hydraulic gradient is insufficient to move the remaining particles inside the specimen.

## 5 CONCLUSIONS

In this study we carried out internal erosion experiments under a horizontal seepage flow using a newly designed apparatus. To detect the movement of the fine particles, we use dyed fine particles in different sections of the soil column to visualize the progress of the erosion process and use a camera to record the loss of particles at the outlet for different erosion times.

Based on the results of the experiments, we found the newly developed apparatus to be reliable for exploring the internal erosion behaviors under horizontal seepage. The experiment reveals that fine particles move within a local range when the hydraulic gradient reaches 0.62. If the hydraulic gradient increases, the global movement and continuous erosion of the fine particles will be triggered. During the early stage of the erosion, particles are rapidly eroded, which then becomes gradual as the erosion progresses. In the horizontal seepage flow, the upper part of the specimen is preferentially eroded, and the dominant seepage area is formed. With the continuation of erosion, the dominant seepage area gradually extends from the upper part to the lower part of the column.

## Acknowledgement

This work was supported by the National Key R&D Program of China (grant numbers 2019YFC1510802 & 2018YFB1600400), the National Natural Science Foundation of Chongqing, China (grant number cstc2018jcyjAX0559), the Innovation Program in water conservancy science and technology of Guangdong China (grant number 2020-13), and the Chongqing Postgraduate Scientific Research Innovation Project(CYB20179).

## 6 REFERENCES

- <sup>1</sup> M. Foster, R. Fell, M. Spannagle, The statistics of embankment dam failures and accidents, *Canadian Geotechnical Journal*, 37 (2000), 1000–1024, doi:10.1139/t00-030
- <sup>2</sup> K. S. Richards, K. R. Reddy, Critical appraisal of piping phenomena in earth dams, *Bull. Eng. Geol. Environ.*, 66 (2007), 381–402, doi:10.1007/s10064-007-0095-0
- <sup>3</sup> L. M. Zhang, Q. Chen, Seepage failure mechanism of the Gouhourockfill dam during reservoir water infiltration, *Soils and Foundation*, 46 (2006), 557–568, doi:10.3208/sandf.46.557
- <sup>4</sup> J. Kai, T. L. Sheng, C. Hong, Upstream movement of piping channel of double-layer dike foundation based on tip hydraulic gradient, *Chinese Journal of Geotechnical Engineering*, 41 (2019) 8, 1–84, doi:10.11779/CJGE2019S1021
- <sup>5</sup> G. Dong, C. Kai, C. Rui, A Simple Approach to Evaluating Leakage Through Thin Impervious Element of High Embankment Dams[J], *Environmental Earth Sciences*, 77 (2018) 25, 11–25, doi:10.1007/s12665-017-7195-3
- <sup>6</sup> Y. Liang, Q. Wei, C. Ma, Experimental study of the anti-seepage characteristics of sidraton particles, *Materials and Technology*, 54 (2020), 829–835, doi:10.17222/mit.2020.040
- <sup>7</sup> L. Yue, C. Jian-sheng, C. Liang, Laboratory tests and analysis on piping in two-stratum dike foundation, *Chinese Journal of Geotechnical Engineering*, 33 (2011), 624
- <sup>8</sup> C. Jiansheng, H. Wenzheng, W. Shuang, Laboratory tests on development of seepage failure of overlying layer during piping of two-stratum dike foundation, *Chinese Journal of Geotechnical Engineering*, 35 (2013), 1777–1783
- <sup>9</sup> K. Vandenboer, L. Dolphen, A. Bezuijen, Backward erosion piping through vertically layered soils, *European Journal of Environmental and Civil Engineering*, 23 (2019), 1404–1412, doi:10.1080/19648189.2017.1373708
- <sup>10</sup> N. Xiaodong, Z. Xiangyu, S. Daming, Study on the Piping Erosion in Levee Foundation by Sand Box Model Test, *Advanced Engineering Sciences*, 50 (2018), 24–31, doi:10.15961jsuese.201700849
- <sup>11</sup> C. Hong, X. Ying-ping, Experimental study of permeability characteristics of surface soil during seepage and deformation, *Rock and Soil Mechanics*, 38 (2017), 2465–2472, doi:10.16285/j.rsm.2017.09.001
- <sup>12</sup> Y. P. Xiao, H. Cao, C. Zhai, Analytical and experimental investigation of a disturbed zone around a pipe in sand, *Journal of the Brazilian Society of Mechanical Sciences & Engineering*, 40 (2018), 1–11, doi:10.1007/s40430-018-1160-2
- <sup>13</sup> Z. Can-hong, Q. Ya-jun, Z. Qi-ming, Permeability characteristics of silty sand under vertical and horizontal seepages, *Chinese Journal of Geotechnical Engineering*, 42 (2020), 163–167, doi:10.11779/CJGE2020S2029
- <sup>14</sup> W. XinZhi, W. Xing, H. MingJian, Study of permeability of calcareous silty layer of foundation at an artificial reclamation island, *Rock and Soil Mechanics*, 11 (2017), 3127–3135, doi:10.16285/j.rsm.2017.11.007
- <sup>15</sup> Q. Licheng, C. Qun, Z. YaJun, Seepage tests on double-layer soils composed of sandy gravel and sand under different stresses and shear displacements, *Chinese Journal of Geotechnical Engineering*, 40 (2018), 63–67, doi:10.11779/CJGE2018S2013
- <sup>16</sup> Z. Li, L. FaYun, W.Chen, Fine soil particle entrainment induced by contact erosion between cohesionless soil layers under horizontal seepage condition, *Engineering Mechanics*, 38 (2021), 143–150, doi:1000-4750(2021)05-0143-08
- <sup>17</sup> M Jiang, Z Shen, J Wang, A novel three-dimensional contact model for granulates incorporating rolling and twisting resistances, *Computers & Geotechnics*, 65 (2015), 147–173, doi:10.1016/j.comgeo.2014.12.011
- <sup>18</sup> ASTM, Standard test method for particle-size analysis of soils, *Annu. B. ASTM Stand.* (2007)
- <sup>19</sup> T. Shire, C. O’Sullivan, K. J. Hanley, Fabric and Effective Stress Distribution in Internally Unstable Soils, *J. Geotech. Geoenviron. Eng.*, 140 (2014), 1–11, doi:10.1061/(ASCE)GT.1943-5606.0001184
- <sup>20</sup> L. Yue, Y. T-C. Jim, C. Qingkong, Particle erosion in suffusion under isotropic and anisotropic stress states, *Soils and Foundations*, 59 (2019), 1371–1384, doi:10.1016/j.sandf.2019.06.009.
- <sup>21</sup> Y. Liang, T. Yeh, C. Ma, Experimental Investigation of Internal Erosion Behaviours in Inclined Seepage Flow, *Hydrological Processes*, 34 (2020), 5315–5326, doi:10.1002/hyp.13944
- <sup>22</sup> E. T. Selig, R. S Ladd, Preparing Test Specimens Using Undercompaction, *Geotechnical Testing Journal*, 1 (1978), 16–23, doi:10.1520/GTJ10364J
- <sup>23</sup> H. Wen-She, F. Duo, Y. JuRui, Study on incipient velocity of sediment, *Journal of hydraulic engineering*, 10 (2002), 51–56
- <sup>24</sup> H. Qiwei, Characteristics of Incipient Sediment Motion and Incipient Velocity, *Journal of Sediment Research*, 2 (1982), 11–26, doi:10.16239/j.cnki.0468-155x.1982.02002
- <sup>25</sup> M. Chang-xi, D. Xiao-bao, On seepage forces and application, *Rock and Soil Mechanics*, 30 (2009), 1569–1574